physica **p** status **S** solidi **S** **rrl**

rapid research letters

6
2019

2 cm

5 µm

200 nm

All-Solution-Processed Micro/Nanowires as Transparent Conducting Electrodes

C. Yang, J. M. Merlo, L. A. D'Imperio, A. H. Rose, Y. M. Calm,
B. Han, J. Gao, G. Zhou, M. J. Burns, K. Kempa, M. J. Naughton

WILEY-VCH

All-Solution-Processed Micro/Nanowires with Electroplate Welding as Transparent Conducting Electrodes

Chaobin Yang, Juan M. Merlo, Luke A. D'Imperio, Aaron H. Rose, Yitzi M. Calm, Bing Han, Jinwei Gao, Guofu Zhou, Michael J. Burns, Krzysztof Kempa, and Michael J. Naughton*

An all-solution-processed transparent conductive electrode with sheet resistance one order of magnitude smaller than conventional nanowire-based transparent conductors has been developed. This is achieved by integrating all-solution produced microwires with a nanowire solution and electroplating and electrowelding. Advantages of the resulting transparent conductor are indium-free, vacuum-free, and lithographic-facility-free, and metallic-mask-free, with small domain size ($\approx 10 \, \mu m^2$), low sheet resistance ($R_s < 1 \, \Omega \, \square^{-1}$), high optical transmittance ($T > 80\%$), mechanical flexibility, and scalability, thus making it an excellent replacement for ITO.

Transparent conductive electrodes (TCEs), which combine high electrical conductivity with high optical transmittance, play a crucial role in numerous modern devices, such as thin film solar cells, flat panel displays, touch screen displays, smart windows, energy harvesters, transparent memory, electromagnetic shielding, heaters, sensors, supercapacitors, and organic light-emitting diodes (OLEDs).[1–12] Among all TCEs, the most successful one is tin-doped indium oxide (ITO). ITO has optical transmittance higher than 80% in the visible range and sheet resistance R_s of about $10 \, \Omega \, \square^{-1}$. In spite of its near ubiquity, ITO suffers from several major drawbacks due to scarcity of the rare earth metal indium, brittleness, and high cost of vacuum-based deposition processes.[2,13] Thus, efforts are underway to seek a replacement for ITO, with intensive investigations of

C. Yang, Dr. J. M. Merlo, L. A. D'Imperio, A. H. Rose, Y. M. Calm,
Dr. M. J. Burns, Prof. K. Kempa, Prof. M. J. Naughton
Department of Physics
Boston College
Chestnut Hill, MA 02467, USA
E-mail: naughton@bc.edu

B. Han, Prof. J. Gao, Prof. K. Kempa
Institute for Advanced Materials
South China Normal University
Guangzhou 510006, China

Prof. G. Zhou, Prof. M. J. Naughton
International Academy of Optoelectronics at Zhaoqing
South China Normal University
Zhaoqing 526238, China

The ORCID identification number(s) for the author(s) of this article can be found under https://doi.org/10.1002/pssr.201900010.

materials such as aluminum-doped zinc oxide (AZO),[14,15] graphene,[16] reduced graphene oxide,[17,18] metal nanowires (MNWs),[19,20] and continuous metallic networks.[21–23] To compare these, it is crucial to consider the cost of materials and the facilities needed for fabrication, and whether vacuum processes are required. Solution processes are preferable to vacuum-based processes due to their lower facilities cost, higher efficiency of material usage, and better scalability.

Among the alternatives for ITO, metallic (e.g., silver,[19] gold,[24] copper[25]) nanowires stand out because they are indium-free, vacuum-free by growing from solution,[26] and can be flexible, thus overcoming most of ITO's drawbacks. Although metals have excellent bulk electrical conductivity, the contact resistance between nanowires dominates the resistivity of TCEs made by MNWs; therefore, nanowire-to-nanowire "welding" is a necessary step after MNW coating (via e.g., drop coating,[19,27] spin coating, spraying,[20] Mayer rod coating,[28] and vacuum-filtering).[29,30] Good welding between nanowires is also essential for mechanical properties of nanowires, and required for foldable and stretchable electronics.[31–34] Researchers have developed various welding methods such as thermal heating,[35] mechanical pressing,[27] chemical welding,[33] plasmonic treatment[36,37] and nano-joining by conductive polymers,[38] conductive nanoparticles[34] or carbon nanomaterials.[39,40]

There are several approaches in the literature for preparing continuous metallic networks that do not require such a welding step: (i) lithographically made patterns followed by vacuum-based metal deposition[41,42]; (ii) lithographically made patterns followed by solution-based metal deposition[21]; and (iii) random self-cracking films as mask followed by vacuum-based metal deposition.[22,43] It is necessary to mention, however, that self-cracking materials used at room temperature and pressure reported to date do not survive solution-based metal deposition. Suh et al.[44,45] reported Si_3N_4 can crack with tensile stress in Si_3N_4/Si systems but (low pressure and high temperature) chemical vapor deposition is used for Si_3N_4 deposition and TCEs made by this method must be transferred to flexible substrates, because Si is not transparent. To eliminate both costly lithographic facilities and costly vacuum-based metal deposition,

some of the current authors previously reported a maskless photolithographic process called crackle photolithography (CPL)[46,47] by replacing a conventional metallic mask with UV-stable self-cracking films. Random photoresist patterns produced by CPL survive solution-based metal deposition and CPL-based TCEs are fully solution-processed and do not require hard lithographic or mask writing facilities.[47] Although continuous metal networks can achieve extremely low sheet resistance ($<0.1\,\Omega\,\square^{-1}$), lower than MNWs by electroplating,[47,48] the domain sizes in all the aforementioned continuous metallic network examples are limited by mask domain size or crackle size, and therefore are larger than for MNWs. For this reason, these metallic networks may be difficult to apply to display products, where there is a drive toward smaller pixel dimensions.

Here, we report the integration of Ag nanowires (AgNWs) with microscale continuous Ag networks made by CPL.[46,47] This combination maintains the qualities of both MNWs and continuous metallic networks, and results in scalable film structures that are flexible, indium-free, vacuum-free, lithographic-facility-free, and metallic-mask-free, with small domain size and high electrical conductivity. Here, silver is chosen because of its chemical stability and excellent conductivity. One can either spin coat Ag nanowires first (NF), then fabricate a microwire network, or reverse the process by fabricating a microwire network first (MF) and then depositing nanowires. One can also solder nanowires to microwires by electrowelding/plating to improve mechanical contact and further lower sheet resistance.

Results and Discussion: **Figure 1** is a schematic of the two different approaches to obtain micro/nanowire TCEs. Panel 1 shows the NF process. A AgNW/isopropyl alcohol (IPA) solution is first spin coated onto a glass substrate and annealed in air at 200 °C. Annealing can provide better contact between AgNWs, and thus lower contact resistance.[35] Next, microwires are produced via CPL (Figure 1(1b–1e)).[46,47] Bis(trimethylsilyl) amine (HMDS) and Shipley S1805 photoresist are spin coated and soft baked to evaporate photoresist solvent. A self-cracking material solution (e.g., nail polish/water solution[43,46,47]) is then spin coated which, upon drying in air at room temperature, self-cracks. TiO$_2$ nanoparticles,[22] CA600 (an acrylic resin water-based dispersion),[22] CYTOP[23] and albumin[48] are also known to crack spontaneously upon drying. To our knowledge, however, none of these self-cracking materials can survive conventional wet processes, so many previous works required vacuum-based metal deposition. Nail polish is particularly useful as a cracking template in CPL because it can block UV light, which makes it an appropriate photoresist mask and, therefore, CPL can avoid the fabrication of a conventional metal mask. After 2 s exposure to 405 nm UV light, only the photoresist not covered by the nail polish gets exposed. Exposed photoresist and nail polish mask will subsequently dissolve in the water-based photoresist developer MF319 and leave randomly cracked photoresist patterns over AgNW-coated glass (Figure 1(1c)). These photoresist patterns are transferred from nail polish; however, they will survive both acidic and alkaline solutions during conventional wet processes, and so can be used as masks for subsequent buffered oxide etch (BOE) and electroless Ag deposition processes. BOE will create ≈1 μm deep channels. The purpose
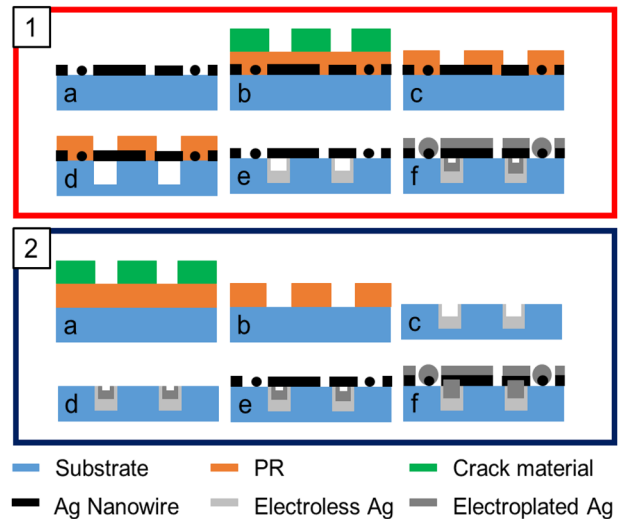

Figure 1. Two different micro/nanowire-based TCE fabrication processes. Method NF, nanowires first: (1a) spin coat AgNWs and bake; (1b) spin coat photoresist and soft bake; spin coat self-cracking material; material self-cracks upon drying in air; (1c) UV expose photoresist (PR); develop photoresist; (1d) etch glass; (1e) electrolessly deposit silver; lift off photoresist; (1f) electroplate silver. Method MF, microwires first: (2a) spin coat and soft bake photoresist followed by spin coat self-cracking material; material self-cracks upon drying in air; (2b) UV expose photoresist; develop photoresist; (2c) etch glass; electrolessly deposit silver; lift off photoresist; (2d) electroplate silver; (2e) spin coat AgNWs; (2f) electroplate silver again.

of BOE here is to activate the glass surface by creating silanol groups,[49] thus increasing adhesion of electrolessly-deposited Ag. Using Tollen's electroless reaction,[50] about 100 nm thick Ag is deposited onto all surfaces. Using lift-off in acetone, the photoresist together with unwanted silver are removed, leaving the Ag microwire network. If desired, additional Ag can be electroplated to increase contact between micro/nanowires and as a result the sheet resistance of the whole sample can be further decreased.

Panel 2 in Figure 1 is the MF process. Microwires are made by the same CPL process above: spin coat and soft bake photoresist, spin coat nail polish which then cracks, UV expose and develop photoresist, BOE etch glass, electrolessly deposit Ag and lift off. Different from the NF process, one extra electroplating step can be done to increase the thickness of microwires before spin coating the nanowires. The electroplated Ag will fill the etched channels first without significantly increasing the microwires' width, thus making the sheet resistance decrease faster than the transmittance decrease. After spin coating Ag nanowires, a second electroplating can also be done for micro/nanowire welding.

Figure 2(a) and (b) show optical images of TCEs on glass substrates made by the NF and MF methods. Corresponding SEM images by the two methods are shown in (c) and (d). One can clearly see nanowires cover the open space between the microwires in both methods. As a result, domain size drops significantly, to ≈10 μm² in micro/nanowires samples. In Figure 2f, a nanowire junction after electroplating (see Figure 1(1f)) is compared with junctions before electroplating
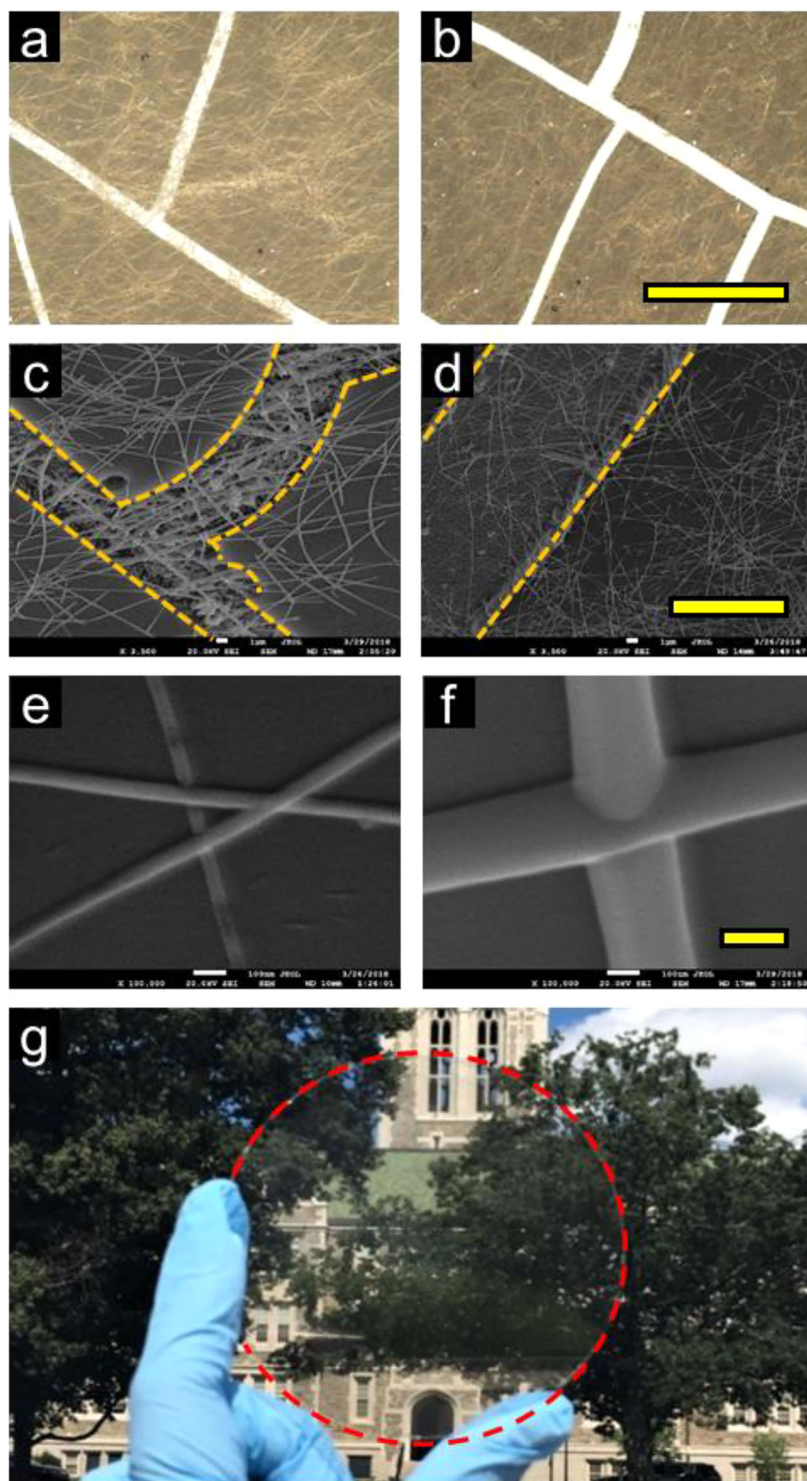
Figure 2. Optical and SEM images of micro/nanowire-based TCEs. a,c) Optical and SEM images of silver micro/nanowires made by NF (Figure 1(1f)). b,d) Corresponding images made by MF (Figure 1(2f)). Dashed lines indicate edges of microwires. e) SEM of junctions between nanowires before eletroplating. f) SEM of a junction between two nanowires after eletroplating. g) Photograph of a 100 mm-diameter glass sample (inside dashed circle) made by MF (Figure 1(2f)), held in front of a building. Scale bars: (b) 100 µm, pertaining also to (a); (d) 10 µm, pertaining also to (c); (f) 200 nm, pertaining also to (e). SEM images taken at 60 degree tilt.

(Figure 2e). Electroplating increases the width of the nanowires and makes two wires embedded into each other, rather than merely touching. This benefits the sheet resistance and only slightly decreases the transmittance. Figure 2g is a photograph of a 100 mm diameter glass substrate coated by micro/nanowires, placed in front of a building, demonstrating both the high transparency and the wafer-scalability of our process.

Electroplating is used in both the NF and MF methods for micro/nanowire welding (see Figure 1(1f and 2f)). Figure S1, Supporting Information demonstrates how the transmittance and sheet resistance of micro/nanowires change by varying electroplate welding time. Transmittance is measured at 550 nm and averaged over five different spots. Both transmittance and sheet resistance are scaled to the same sample before electroplate welding. Electroplate welding decreases transmittance and sheet resistance because micro/nanowire width increases. It is interesting to note that in the first 20 s, sheet resistance drops fastest. The reason is that nanowire junctions change from "touching" to "embedded" in this timeframe, as shown in Figure 2f. Because longer electroplating time can decrease transmittance and the decrease of sheet resistance saturates after 20 s, we chose 20 s for the electroplate welding time for both NF and MF micro/nanowires.

Particularly for the MF method, electroplating is used to increase Ag microwire thickness (Figure 1(2d)). Previous work has used electroplating to increase the conductivity of TCEs and has achieved good results,[48] but there remains one drawback: electroplated Ag grows in all directions, so the increasing widths of Ag metallic wires will decrease transmittance. The CPL process solves this problem by electroplating the silver within the etched channels, which largely constrain the microwire widths to the channel widths.[46,47] Thus, one can use relative longer electroplating time (e.g., 50 s) to increase the microwire thickness and reduce the sheet resistance by one order of magnitude without appreciably changing optical transmittance.

The domain size of the nail polish crack pattern can be controlled by spin speeds of the nail polish solution. In Figure S2, Supporting Information, we show optical microscope images of micro/nanowires made by the MF method using spin speeds from 2000 to 5000 rpm. The performance of samples made by all speeds is shown in **Figure 3**a, indicated by different colors. Each color has four points and from right to left they are: before the first electroplating (Figure 1(2c)); after the first electroplating (Figure 1(2d)); after spin coating
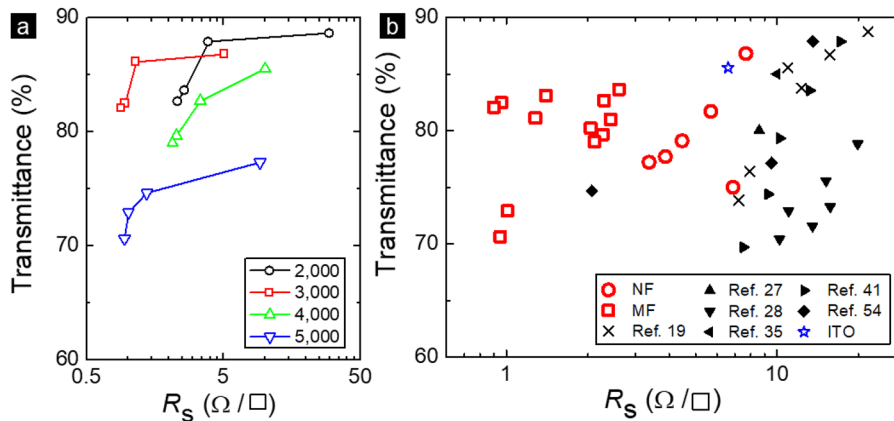
Figure 3. TCEs made by MF and NF, and their performance. a) T and R_s of MF samples made by spin coating nail polish solution at speeds from 2000 to 5000 rpm. For each set of data, points from right to left represent performance before first electroplating (Figure 1(2c)), after first electroplating (Figure 1 (2d)), after spin coating AgNWs (Figure 1(2e)) and after second electroplating (Figure 1(2f)). b) T versus R_s for TCEs made by the current NF (circles) and MF (squares) methods. Results from other silver nanowire approaches, as well as commercial ITO (star), are included for comparison.

Ag nanowires (i.e., before the second electroplating, Figure 1 (2e)); after the second electroplating (Figure 1(2f)). First, one can see lower nail polish spin speed yields larger domain sizes and lower microwire metal coverage, and thus higher transmittance, which is consistent with our previous CPL work.[47] Second, among all steps adding Ag to samples, the first electroplating, which the NF process does not have, decreases sheet resistance the most and this electroplating step turns out to be the reason that MF samples outperform NF samples.

A figure of merit (FoM) is often used to compare the performance of TCEs prepared by various methods. Haacke[51] proposed to use $\phi = T^{10}/R_s$, which puts heavy weight on transmittance T and has units of Ω^{-1}. Another popular one is the ratio of electrical conductance to optical conductance ($F_{TCE} = \sigma_{dc}/\sigma_{op}$) which can be written as $F_{TCE} = Z_o/\{2R_s(T^{-1/2} - 1)\}$, where $Z_O = \sqrt{\mu_O/\varepsilon} \approx 377\,\Omega$ is the impedance of free space, R_s is

sheet resistance and T is transmittance at 550 nm.[30,41,52,53] We use both ϕ and F_{TCE} here to compare our result in Figure 3b with various AgNWs from other work. Our NF results shown as red circles (F_{TCE} up to 404, $\phi = 0.03$) are slightly better than almost all previous works, including those that deposit AgNWs by drop coating (crosses, $F_{TCE} = 211$, $\phi = 0.02$)[19] and by Mayer rod coating (down triangles, $F_{TCE} = 100$, $\phi = 0.0046$).[28] They are also superior to those that weld AgNWs by solution methods (mechanical pressing: up triangles, $F_{TCE} = 186$, $\phi = 0.012$[27]; thermal heating: left triangles, $F_{TCE} = 223$, $\phi = 0.02$[35]) and even lithography made nanogrids (right triangles, $F_{TCE} = 164$, $\phi = 0.016$)[41]. The FoM of our MF samples (red squares, F_{TCE} up to 2016, $\phi = 0.153$) is also higher than that of a micro/nanowires process made by photolithography (diamonds, $F_{TCE} = 579$, $\phi = 0.026$).[54] For reference, commercial ITO (blue star) has an $F_{TCE} = 350$ and $\phi = 0.03$.
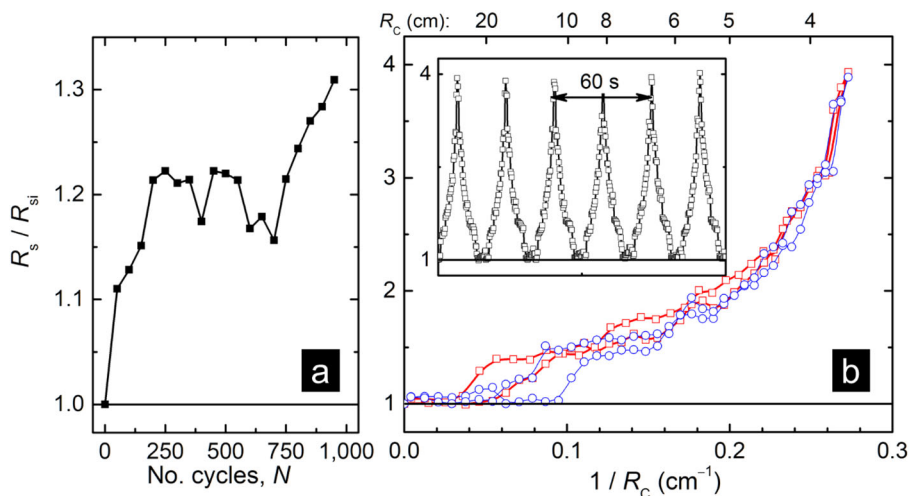

Figure 4. Sheet resistance of MF sample measured while bending. a) R_s over the first 1000 bending cycles, scaled to initial, unbent value. Each point is an average from 50 bending cycles divided by sheet resistance before bending. b) Scaled R_s versus inverse radius of curvature for two bending cycles. Inset: Scaled R_s during first six bending cycles.

Many applications of TCEs require mechanical flexibility. Our micro/nanowires can be transferred to flexible substrates, such as polyethylene terephthalate (PET). **Figure 4** shows results from bending tests of the MF micro/nanowires on PET substrates. Figure 4a shows how sheet resistance changes in the first 1000 bending cycles. Each point in the figure is the average of the measured sheet resistance data over 50 cycles, scaled to the initial, unbent value R_{si}. After 1000 of these ≈90 degree bends, the resistance was about 30% higher than the initial value, indicating some chronic changes to the network. Figure 4b shows how sheet resistance changes in each cycle, wherein the scaled R_s increases by up to 300% at maximum bend but, at least for these first few bends (inset), largely recovers when unbent. We plot the data in Figure 4b against radius of curvature, indicating the ability of these flexible films to be bent to a few centimeters radius. The data in Figure 4 were measured by the 4-probe van der Pauw method.

In conclusion, we have demonstrated two variants of an all-solution method to produce Ag micro/nanowire films as transparent conductors. By integrating crackle photolithography-based microwires with nanowires and electroplate welding, we obtain transparent conductors with $R_s < 1\,\Omega\,\square^{-1}$, $T > 80\%$, and domain size ≈10 μm². We also showed that samples can be transferred to flexible substrates, making a possible cost-effective candidate for flexible applications. Future effort will be devoted to more fully characterizing the details of the structural changes associated with flexing the films, toward minimizing such resistance changes.

Supporting Information

Supporting Information is available from the Wiley Online Library or from the author.

Conflict of Interest

The authors declare no conflict of interest.

Keywords

electroplating, nanowires, solution process, transparent conducting electrodes, welding

[1] B. Han, Q. Peng, R. Li, Q. Rong, Y. Ding, E. M. Akinoglu, X. Wu, X. Wang, X. Lu, Q. Wang, G. Zhou, J.-M. Liu, Z. Ren, M. Giersig, A. Herczynski, K. Kempa, J. Gao, *Nat. Commun.* **2016**, *7*, 12825.

[2] J. Gao, K. Kempa, M. Giersig, E. M. Akinoglu, B. Han, R. Li, *Adv. Phys.* **2016**, *65*, 553.

[3] T. Sannicolo, M. Lagrange, A. Cabos, C. Celle, J.-P. Simonato, D. Bellet, *Small* **2016**, *12*, 6052.

[4] V. Oddone, M. Giersig, *Phys. Status Solidi RRL* **2017**, *11*, 1700005.

[5] J. Xiong, S. Li, Y. Ye, J. Wang, K. Qian, P. Cui, D. Gao, M.-F. Lin, T. Chen, P. S. Lee, *Adv. Mater.* **2018**, *30*, 1802803.

[6] H. Lu, X. Ren, D. Ouyang, W. C. H. Choy, *Small* **2018**, *14*, 1703140.

[7] C. K. Jeong, J. Lee, S. Han, J. Ryu, G.-T. Hwang, D. Y. Park, J. H. Park, S. S. Lee, M. Byun, S. H. Ko, K. J. Lee, *Adv. Mater.* **2015**, *27*, 2866.

[8] J. H. Park, S. Han, D. Kim, B. K. You, D. J. Joe, S. Hong, J. Seo, J. Kwon, C. K. Jeong, H.-J. Park, T.-S. Kim, S. H. Ko, K. J. Lee, *Adv. Funct. Mater.* **2017**, *27*, 1701138.

[9] J. Jung, H. Lee, I. Ha, H. Cho, K. K. Kim, J. Kwon, P. Won, S. Hong, S. H. Ko, *ACS Appl. Mater. Interfaces* **2017**, *9*, 44609.

[10] S. Hong, H. Lee, J. Lee, J. Kwon, S. Han, Y. D. Suh, H. Cho, J. Shin, J. Yeo, S. H. Ko, *Adv. Mater.* **2015**, *27*, 4744.

[11] K. K. Kim, S. Hong, H. M. Cho, J. Lee, Y. D. Suh, J. Ham, S. H. Ko, *Nano Lett.* **2015**, *15*, 5240.

[12] H. Lee, S. Hong, J. Lee, Y. D. Suh, J. Kwon, H. Moon, H. Kim, J. Yeo, S. H. Ko, *ACS Appl. Mater. Interfaces* **2016**, *8*, 15449.

[13] K. Ellmer, *Nat. Photonics* **2012**, *6*, 809.

[14] T. Minami, H. Nanto, S. Takata, *Jpn. J. Appl. Phys.* **1984**, *23*, L280.

[15] H. Kim, C. M. Gilmore, *Appl. Phys. Lett.* **2000**, *76*, 259.

[16] S. Bae, H. Kim, Y. Lee, X. Xu, J.-S. Park, Y. Zheng, J. Balakrishnan, T. Lei, H. R. Kim, Y. I. Song, Y.-J. Kim, K. S. Kim, B. Özyilmaz, J.-H. Ahn, B. H. Hong, S. Lijima, *Nat. Nanotechnol.* **2010**, *5*, 574.

[17] G. Eda, G. Fanchini, M. Chhowalla, *Nat. Nanotechnol.* **2008**, *3*, 270.

[18] Z. Yin, S. Wu, X. Zhou, X. Huang, Q. Zhang, F. Boey, H. Zhang, *Small* **2010**, *6*, 307.

[19] J.-Y. Lee, S. T. Connor, Y. Cui, P. Peumans, *Nano Lett.* **2008**, *8*, 689.

[20] V. Scardaci, R. Coull, P. E. Lyons, D. Rickard, J. N. Coleman, *Small* **2011**, *7*, 2621.

[21] B. Sciacca, J. van de Groep, A. Polman, E. C. Garnett, *Adv. Mater.* **2016**, *28*, 905.

[22] B. Han, K. Pei, Y. Huang, X. Zhang, Q. Rong, Q. Lin, Y. Guo, T. Sun, C. Guo, D. Carnahan, M. Giersig, Y. Wang, J. Gao, Z. Ren, K. Kempa, *Adv. Mater.* **2014**, *26*, 873.

[23] Z. Xian, B. Han, S. Li, C. Yang, S. Wu, X. Lu, X. Gao, M. Zeng, Q. Wang, P. Bai, M. J. Naughton, G. Zhou, J.-M. Liu, K. Kempa, J. Gao, *Adv. Mater. Technol.* **2017**, *2*, 1700061.

[24] P. E. Lyons, S. De, J. Elias, M. Schamel, L. Philippe, A. T. Bellew, J. J. Boland, J. N. Coleman, *J. Phys. Chem. Lett.* **2011**, *2*, 3058.

[25] A. R. Rathmell, S. M. Bergin, Y.-L. Hua, Z.-Y. Li, B. J. Wiley, *Adv. Mater.* **2010**, *22*, 3558.

[26] Y. Sun, B. Gates, B. Mayers, Y. Xia, *Nano Lett.* **2002**, *2*, 165.

[27] T. Tokuno, M. Nogi, M. Karakawa, J. Jiu, T. T. Nge, Y. Aso, K. Suganuma, *Nano Res.* **2011**, *4*, 1215.

[28] L. Hu, H. S. Kim, J.-Y. Lee, P. Peumans, Y. Cui, *ACS Nano* **2010**, *4*, 2955.

[29] Z. C. Wu, Z. H. Chen, X. Du, J. M. Logan, J. Sippel, M. Nikolou, K. Kamaras, J. R. Reynolds, D. B. Tanner, A. F. Hebard, A. G. Rinzler, *Science* **2004**, *305*, 1273.

[30] S. De, T. M. Higgins, P. E. Lyons, E. M. Doherty, P. N. Nirmalray, W. J. Blau, J. J. Boland, J. N. Coleman, *ACS Nano* **2009**, *3*, 1767.

[31] Y. Won, A. Kim, W. Yang, S. Jeong, J. Moon, *NPG Asia Mater.* **2014**, *6*, e132.

[32] P. Lee, J. Lee, H. Lee, J. Yeo, S. Hong, K. H. Nam, D. Lee, S. S. Lee, S. H. Ko, *Adv. Mater.* **2012**, *24*, 3326.

[33] S. J. Lee, Y.-H. Kim, J. K. Kim, H. Baik, J. H. Park, J. Lee, J. Nam, J. H. Park, T.-W. Lee, G.-R. Yi, J. H. Cho, *Nanoscale* **2014**, *6*, 11828.

[34] S.-P. Chen, Y.-C. Liao, *Phys. Chem. Chem. Phys.* **2014**, *16*, 19856.

[35] A. Madaria, A. Kumar, F. Ishikawa, C. Zhou, *Nano Res.* **2010**, *3*, 564.

[36] E. C. Garnett, W. S. Cai, J. J. Cha, F. Mahmood, S. T. Connor, M. G. Christoforo, Y. Cui, M. D. McGehee, M. L. Brongersma, *Nat. Mater.* **2012**, *11*, 241.

[37] S. Han, S. Hong, J. Ham, J. Yeo, J. Lee, B. Kang, P. Lee, J. Kwon, S. S. Lee, M.-Y. Yang, S. H. Ko, *Adv. Mater.* **2014**, *26*, 5808.

[38] J. Lee, P. Lee, H. B. Lee, S. Hong, I. Lee, J. Yeo, S. S. Lee, T.-S. Kim, D. Lee, S. H. Ko, *Adv. Funct. Mater.* **2013**, *23*, 4171.

[39] S.-T. Hsiao, H.-W. Tien, W.-H. Liao, Y.-S. Wang, S.-M. Li, C.-C. MMa, Y.-H. Yub, W.-P. Chuang, *J. Mater. Chem. C* **2014**, *2*, 7284.

[40] P. Lee, J. Ham, J. Lee, S. Hong, S. Han, Y. D. Suh, S. E. Lee, J. Yeo, S. S. Lee, D. Lee, S. H. Ko, *Adv. Funct. Mater.* **2014**, *24*, 5671.

[41] J. van de Groep, P. Spinelli, A. Polman, *Nano Lett.* **2012**, *12*, 3138.

[42] J. van de Groep, D. Gupta, M. A. Verschuuren, M. M. Wienk, R. A. J. Janssen, A. Polman, *Sci. Rep.* **2015**, *5*, 11414.

[43] K. D. M. Rao, R. Gupta, G. U. Kulkarni, *Adv. Mater. Interfaces* **2014**, *1*, 1400090.

[44] Y. D. Suh, J. Kwon, J. Lee, H. Lee, S. Jeong, D. Kim, H. Cho, S. H. Ko, *Adv. Electron. Mater.* **2016**, *2*, 1600277.

[45] Y. D. Suh, S. Hong, J. Lee, H. Lee, S. Jung, J. Kwon, H. Moon, P. Won, J. Shin, J. Yeo, S. H. Ko, *RSC Adv.* **2016**, *6*, 57434.

[46] M. J. Naughton, C. Yang, K. Kempa, M. J. Burns, *All Solution-Process and Product for Transparent Conducting Film*, **2017**, U.S. Patent Application No. 15/455,762.

[47] C. Yang, J. M. Merlo, J. Kong, Z. Xian, B. Han, G. Zhou, J. Gao, M. J. Burns, K. Kempa, M. J. Naughton, *Phys. Status Solidi A* **2017**, *215*, 1700504.

[48] Q. Peng, S. Li, B. Han, Q. Rong, X. Lu, Q. Wang, M. Zeng, G. Zhou, J.-M. Liu, K. Kempa, J. Gao, *Adv. Mater. Technol.* **2016**, *1*, 1600095.

[49] N. Chitvoranund, S. Jiemsirilers, D. P. Kashima, *J. Aust. Ceram. Soc.* **2013**, *49*, 62.

[50] *CRC Handbook of Chemistry and Physics* (Ed: W. M. Haynes), CRC Press, Boca Raton, FL, USA **2016**.

[51] G. Haacke, *J. Appl. Phys.* **1976**, *47*, 4086.

[52] M. Dressel, G. Grüner, *Electrodynamics of Solids: Optical Properties of Electrons in Matter*. Cambridge University Press, Cambridge, UK **2002**.

[53] L. Hu, D. S. Hecht, G. Grüner, *Nano Lett.* **2004**, *4*, 2513.

[54] J. Jang, H.-G. Im, J. Jin, J. Lee, J.-Y. Lee, B.-S. Bae, *ACS Appl. Mater. Interfaces* **2016**, *8*, 27035.

Supporting Information

All-solution-processed micro/nanowires with electroplate welding as transparent conducting electrodes

Chaobin Yang, Juan M. Merlo, Luke A. D'Imperio, Aaron H. Rose, Yitzi M. Calm, Bing Han, Jinwei Gao, Guofu Zhou, Michael J. Burns, Krzysztof Kempa and Michael J. Naughton*

C. Yang, Dr. J. M. Merlo, L. A. D'Imperio, A. H. Rose, Y. M. Calm, Dr. M. J. Burns, Prof. K. Kempa, Prof. M. J. Naughton
Department of Physics, Boston College, Chestnut Hill, Massachusetts 02467, USA
E-mail: naughton@bc.edu (M. J. Naughton)

B. Han, Prof. J. Gao, Prof. K. Kempa
Institute for Advanced Materials, South China Normal University, Guangzhou, 510006, China

Prof. G. Zhou, Prof. M. J. Naughton
International Academy of Optoelectronics, South China Normal University, Zhaoqing, 526238, China
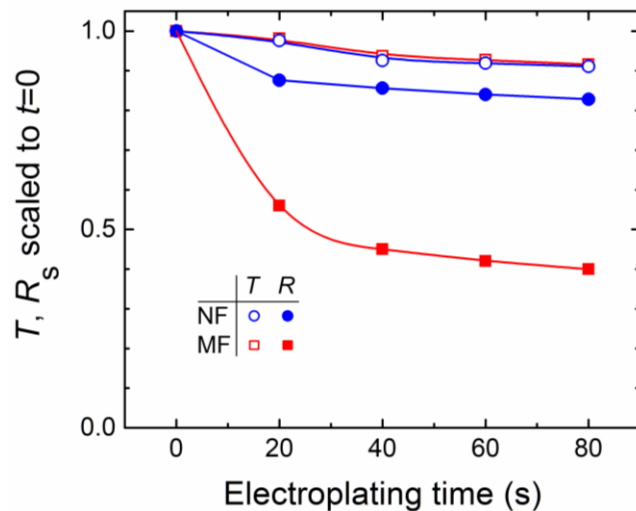
Figure S1. Optical transmittance T and sheet resistance R_s of samples prepared by NF (blue) and MF (red) vs. electroplate welding time. T (hollow) and R_s (filled) are relative to the same sample before electroplating. R_s is measured by the 4-probe van der Pauw method. Lines are guides to the eye.
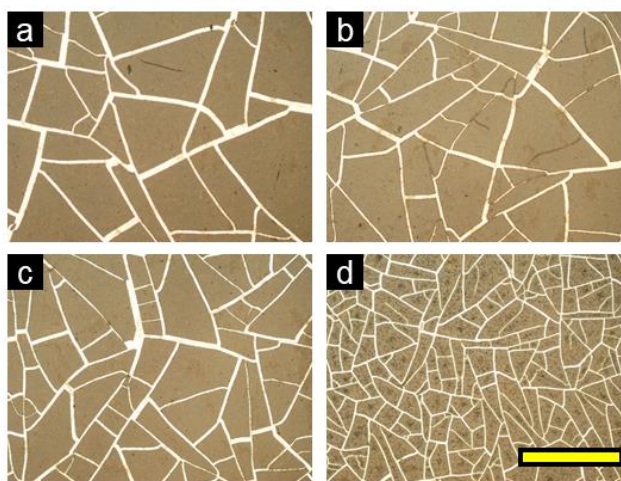

Figure S2. Optical images of micro/nanowire-based TCEs made by MF. (a) - (d) optical microscope images of MF samples made by spin coating nail polish solution at speeds from 2,000 to 5,000 rpm. Scale bar for 500 μm in (d) pertains to all four images.

Experimental Section

Preparation of substrates: Glass substrates in two types of sizes are used. One were 25×25 mm^2, 1.1 mm thick glass substrates and the other were 100 mm diameter, 0.6 mm thick soda lime glass wafers (University Wafer No. 1631). Polyethylene terephthalate (PET) substrates cut into 40×40 mm^2 were used for flexible sample. All substrates were first sonicated in acetone for 10 minutes, followed by another 10 minute sonication in isopropyl alcohol (IPA), and then dried by blowing nitrogen gas.

Preparation of AgNW films: A 20 mg ml^{-1} AgNW-IPA solution (ACS Material no. Agnw-L70) was first diluted 10 times by IPA to 2 mg ml^{-1}. AgNWs have ≈70 nm diameter and 100 - 200 μm length. The cross-section of silver nanowires is pentagonal and there is no capping layer on them. The AgNW-IPA solution was spin coated on glass at 500 rpm for 10 s and then 3,000 rpm for 30 s. The coated substrates were baked on a hot plate at 200 °C for 5 minutes.

Preparation of the cracked photoresist on glass: HDMS (Ultra Pure Solutions, Inc) and positive photoresist Microposit^{TM} S1805 (Dow Chemical Co.) were both spin-coated at 1,000 rpm for 15 s and then 4,000 rpm for 45 s. The coated substrates were baked on a hot plate at 110 °C for 1 min. Nail polish (Qian Zhi Xiu Co., Shenzhen, China) and deionized (DI) water were mixed with volume ratio 5:1. The diluted nail polish was spin coated for 15 s at 500 rpm and for 45 s at speeds between 2,000 rpm and 5,000 rpm, depending of the domain size desired. The samples were then allowed to dry in air for 5 minutes after the nail polish. They were then UV flood exposed (USHIO USH-350DS) for 2 s and developed in Microposit^{TM} MF-319 (Dow Chemical Co.) for 1 minute. Samples were rinsed in DI water for 5 minutes and dried with nitrogen gas.

Silver electroless deposition: The backs of the glass substrates were covered with tape to protect them from the buffered oxide etch (BOE) and Ag electroless deposition processes. Samples were

placed in BOE solution (7:1 volume ratio of 40% NH_4F in water to 49% HF in water, J.T. Baker Chemicals) for 2 minutes. After BOE, the samples were rinsed in water for 5 minutes. The Tollens' reagent process used a solution made by mixing a 60 mL of 0.1 M silver nitrate (Sigma-Aldrich Corp.) solution with a 30 mL, 0.8 M potassium hydroxide (J.T. Baker) solution. The aqueous salt $AgNO_3$ was converted to silver oxide (Ag_2O) by OH^- ions and a brown precipitate formed. Ag_2O was then dissolved by adding ammonium hydroxide (J.T. Baker) dropwise, with stirring and aqueous $[Ag(NH_3)_2]^+$ formed. The $[Ag(NH_3)_2]^+$ complex was reduced by adding a 6 mL, 0.25 M dextrose solution (Fisher Scientific), which contained aldehyde groups. The etched glass samples were placed at the same time with the dextrose solution into a beaker for two minutes, under continuous stirring. The above volumes of solution were suitable for electroless deposition of a 25×25 mm^2 sample. One can increase the volumes of all solutions proportionally for larger samples. The tape was removed from the substrate back before lifting off photoresist and unwanted silver in acetone for 5 minutes.

Silver electroplating: A constant current of 5 mA (Gamry Instruments, Inc., Interface 1000 system) was applied across the silver network cathode and silver plating anode (Esslinger & Co.), placed face-to-face in ready-to-use silver plating solution (Krohn Industries, Inc.). The silver anode was sonicated in acetone and IPA for 10 minutes before use.

Preparation of flexible samples: UV glue (optically clear liquid adhesive by Octopus Glue) was dropped to the surfaces of micro/nanowire-coated glass samples. PET substrates were used to cover the UV glue and then samples were UV exposed for 10 minutes to solidify the glue. These samples were then etched in BOE for 8 hours to remove the glass substrates, leaving the micro/nanowires on UV glue-coated PET substrates.

Characterization: An optical microscope (Olympus BX61) and scanning electron microscope (JEOL JCM-6000) were used to characterize the samples. Sheet resistances were measured by the van der Pauw method. A current source (Keithley 224) and volt meter (Keithley 175A) were connected to samples using silver paste to four corners. Optical transmittance was measured by using an integrating sphere system (Ocean Optics Spectroclip-TR) with a halogen light source (Ocean Optics HL-2000-FHSA) and spectrometer (Ocean Optics Maya 2000 Pro). All transmittance data presented are normalized to that of a clean, glass substrate. The standard deviation of transmittance among different spots on the same sample is around 1% and the variance of the sheet resistance among multiple measurements is less than 1%. The performance of aluminosilicate glass coated by 175 nm ITO (Delta Technologies, LTD., No. CB-40IN-0107) was compared with all other TCEs.